

Geophysical Research Letters[®]

RESEARCH LETTER

10.1029/2022GL099481

Key Points:

- A risk was identified for a very intense and localized precipitation event using a mesoscale operational weather prediction model
- We relate the risk level of a heavy-precipitation event to climate change
- The risk of occurrence of a very heavy precipitation increases with the level of warming

Supporting Information:

Supporting Information may be found in the online version of this article.

Correspondence to:

D. Matte,
matte.dominic@ouranos.ca

Citation:

Matte, D., Christensen, J. H., Feddersen, H., Vedel, H., Nielsen, N. W., Pedersen, R. A., & Zeitzen, R. M. K. (2022). On the potentials and limitations of attributing a small-scale climate event. *Geophysical Research Letters*, 49, e2022GL099481. <https://doi.org/10.1029/2022GL099481>

Received 6 MAY 2022

Accepted 27 JUL 2022

Author Contributions:

Conceptualization: Jens H. Christensen

Data curation: Dominic Matte, Henrik Feddersen

Formal analysis: Dominic Matte, Henrik Feddersen, Henrik Vedel

Methodology: Dominic Matte, Jens H. Christensen, Henrik Feddersen, Henrik Vedel

Visualization: Dominic Matte, Rune M. K. Zeitzen




Writing – original draft: Dominic Matte, Jens H. Christensen, Henrik Feddersen, Henrik Vedel, Niels

Woetmann Nielsen, Rasmus A. Pedersen

© 2022. The Authors.

This is an open access article under the terms of the [Creative Commons Attribution-NonCommercial-NoDerivs License](https://creativecommons.org/licenses/by/4.0/), which permits use and distribution in any medium, provided the original work is properly cited, the use is non-commercial and no modifications or adaptations are made.

On the Potentials and Limitations of Attributing a Small-Scale Climate Event

Dominic Matte^{1,2} , Jens H. Christensen^{1,3} , Henrik Feddersen⁴, Henrik Vedel⁴, Niels Woetmann Nielsen⁴, Rasmus A. Pedersen⁴ , and Rune M. K. Zeitzen¹

¹Physics of Ice, Department of Climate and Earth, Niels Bohr Institute, University of Copenhagen, Copenhagen, Denmark, ²Ouranos, Montréal, QC, Canada, ³NORCE, Norwegian Research Centre AS, Bjerknes Centre for Climate Research, Bergen, Norway, ⁴Danish Meteorological Institute, Copenhagen Ø, Denmark

Abstract Intense convective storms can be hazardous when occurring over large populated cities. In a changing climate, decision makers and the general public increasingly need to be able to better understand if and to what extent these storms are influenced by anthropological climate change and what to expect as climate continues to warm. Unfortunately due to their limited ability to resolve small-scale features in models, convective storms remain a challenge to the modeling community. Here, we use a forecast-ensemble based method using a convection permitting model with full data-assimilation, to assess the risk of exceeding certain precipitation thresholds related to a critical cloudburst event that occurred over Copenhagen, Denmark. Our results show that this set-up is representing well the overall observed intensities. By adapting a pseudo-global warming approach, we show that both the risk for flooding and the risk for reaching unprecedented precipitation intensity increases resulting from further warming.

Plain Language Summary Cloudburst events are extremely damaging, especially when they hit a city center such as the one impacting Copenhagen, Denmark on 2 July 2011. When something like this happens, the public awareness immediately rises, and many questions emerge such as for example, “How is this related to climate change?” Attributing climate change to these kinds of events is challenging since sensitivity to the initial and driving conditions completely undermine state-of-the-art attribution endeavors to address climate change. Here, by addressing different global warming levels we are taking an alternative modeling approach to study such a cloudburst. Specifically, we simulated this event using an esteemed state-of-the-art numerical weather prediction modeling system currently in use at multiple national weather services in Europe. In this study, using a storyline approach, we show that both the risk for flooding and the risk for reaching unprecedented precipitation intensities increase as climate warms. Specifically, we here demonstrate that the risk of occurrence of such an event is found to be almost double to what could have been realized without anthropogenic warming present.

1. Introduction

A cloudburst is the result of strong convective mechanisms. Due to its intensity, suddenness and brief duration, it is particularly difficult to adequately drain the resulting surface water, which accordingly may lead to severe flooding and consequently large economic losses. Such flash floods are not uncommon across the world and are devastating when occurring in a densely populated city such as Copenhagen, Denmark—even without additional complicating runoff effects from surrounding more elevated areas (Khajehi et al., 2020; Ricchi et al., 2021). Predicting the precise location, timing and intensity of weakly forced convective events (e.g., initiated by local surface conditions) is notoriously difficult, even for a state-of-the-art, convection permitting Numerical Weather Prediction (NWP) models due to a combination of (a) model resolution not fully resolving either the deep convection mechanism or local interactions related to orography or land/sea contrasts, (b) imprecise depiction of the initial conditions (IC) due to a lack of high-resolution observations (in particular of humidity) and (c) the chaotic behavior and associated sensitivity to IC of the atmosphere in general and convection in particular (Coppola et al., 2020; Fowler et al., 2021; Olsson et al., 2021; Prein et al., 2015, 2021). If the synoptic scale or orographic forcing is weak, the sensitivity to the IC undermines any hope of using a single deterministic approach to realistically capture the exact location with a risk of occurrence for such an event well in advance, even when the system is embedded within a well depicted synoptic-scale weather system (Bachmann et al., 2020; Hagelin et al., 2017; Schellander-Gorgas et al., 2017).

Writing – review & editing: Dominic Matte, Jens H. Christensen, Henrik Feddersen, Henrik Vedel, Niels Woetmann Nielsen, Rasmus A. Pedersen, Rune M. K. Zeitzen

Recently the IPCC (Masson-Delmotte et al., 2021) concluded that it is difficult to detect and attribute changes in severe convective storms and, therefore, there is limited evidence to support that extreme precipitation associated with severe convective storms has indeed increased from the pre-industrial era. From a climate change attribution perspective, the burden of the computational load related to the resolution needed for simulating such events is particularly challenging. For example, such events are meteorologically unique meaning that they are caused by a unique combination of several mechanisms (Otto & Members of the Climate Science Communications Group, 2019) from local to synoptic scale, which limits the possibility of finding a complete or even similar analog in long, continuous simulations. Consequently, previous studies have explored alternative methods for studying climate change impacts on convective events. There are commonly two approaches: event-driven (Armon et al., 2022; Hibino et al., 2018; Kawase et al., 2020, 2021; Lackmann, 2013; Takayabu et al., 2015) and climatological (Kawase et al., 2019; Lenderink et al., 2021; Liu et al., 2017; Prein, Rasmussen, et al., 2017). The former focuses on the study of a specific event under different conditions related to climate change, while the latter focuses on the general changes of this type of event on a climatological time scale. By construction the climatological approach does not allow comparison of two identical synoptic patterns in different climatic states, which undermines the attribution reasoning. For example, Kawase et al. (2019) used the climatological approach by removing the observed warming trend from the lower boundary condition and investigated climate simulations with and without this trend by addressing all precipitation events, rather than looking at any specific heavy precipitation events. Such an approach makes sense for studying one type of event associated with climate change but would make an event-to-event comparison impossible since no temporal correlation is to be expected between the two data sets.

Although the event-based approach seems more suitable for attribution, it also has several modeling pitfalls (where several of them are also discussed in Leach et al., 2021). The main reason is that extreme events are synoptically unique. They represent an optimal interaction synchronization of unique different meteorological and climatological drivers. One usual approach is to modify those conditions by those expected in warmer or colder climate using for example, a pseudo-global warming (PGW) approach (Schär et al., 1996). However, modifying the state of these singular conditions might well change the extremity of the event itself, especially if it is a convective event where the vertical structure is crucial. In other words, such changes obscure the interpretation of the results. Several studies (Armon et al., 2022; Hibino et al., 2018; Kawase et al., 2020, 2021; Pall et al., 2017) have found that there is a decrease in convective and/or total rainfall amounts in simulations where a PGW approach was applied. It is unclear if this is associated with a change in vertical structure that may dampen the convective mechanisms associated with the original event as it was proposed by for example, Hibino et al. (2018). In this latter study the authors identified a stabilizing effect in the troposphere due to the future temperature change profile enforced by the PGW approach. In order to evaluate this stabilization effect, they run an additional experiment using a vertically uniform set of anomalies, which has a neutral impact on the initial convective instabilities. Using this set-up, they demonstrated an increase in convection and in the precipitation rate with warming.

On the other hand, some studies using a PGW approach did show an increase of precipitation due to an enhanced convective mechanisms (e.g., Attema et al., 2014; Lackmann, 2013). For example, to avoid the stabilization effect, Attema et al. (2014) selected only the future cases with the highest convective available potential energy to modify their profile (which resembles a constant warming profile as noted also Loriaux et al., 2013). This indicate that one additional piece of the puzzle concerns not only the type of event but also how and where a PGW is applied. The different mechanisms may impact the PGW results and analysis. For example, large-scale driven systems such as tropical cyclones (Patricola & Wehner, 2018) are different in comparison to flash-flood events, such as the one presented in this study.

Here, we take a storyline approach (Hazeleger et al., 2015; Shepherd et al., 2018) by applying what is called a methodology based on *climate and weather models* (National Academies of Sciences & Medicine, 2016) to study how a small-scale flash flood event would evolve on a potential (past or) future day with otherwise similar synoptic/large-scale conditions. Note that we do not take a climatological perspective, meaning that we do not study how warming affects the probability of occurrence of this type of event but rather how warming has (and may) affected the intensity of a specific event. First, to address the convective nature of the event, we use a convection permitting regional model that has a demonstrated ability to simulate sub-hourly precipitation intensities with accuracy, when particular care is taken to initialization of the model through a proper data-assimilation (Bengtsson et al., 2017). Next, we overcome the location challenge related to the simulated downpour, by taking

an ensemble approach in combination with a new index defining the risk of exceeding a certain precipitation intensity level (hereinafter simply called the risk index, see Section 2.3 for details). In the particular case, we apply this methodology with the aim to attribute a severe flash flood event to climate change and in addition portray the rising risk index for a similar event should it occur under further global warming. To show the influence of climate change, we adapt and apply a PGW approach (see Section 3.2 for details), to investigate the risk index under different warming levels. Using this event-based set-up, we overcome the scarcity challenge and, furthermore, can assess how the risk index (as defined in Section 2.3) associated with the event change with warming level. The event was a deep moist convection event (see Section 1 of the Supporting Information S1 for a detailed description) taking place over Copenhagen, Denmark in July 2011 and afterward led to insurance claims exceeding 800 million Euro (Arnbjerg-Nielsen et al., 2015) and during the event major infrastructure came at great risk of total failure. Greater hospitals, Rigshospitalet and Hvidovre Hospital, had begun planning the evacuation of all 1,400 bedridden patients, as the power supply and emergency generators (located in the basement) were seriously threatened and were only centimeters of extra water from failure (Newspaper BT (in danish) <https://www.bt.dk/danmark/hospitaler-var-centimeter-fra-katastrofe>).

2. Materials and Methods

2.1. Model Set-Up and Domains of Interest

For this study, we use the HARMONIE-AROME limited-area numerical weather prediction model at 2.5 km grid-mesh with full data-assimilation (Bengtsson et al., 2017). For this cloudburst event, we have used HarmonEPS configuration (Frogner et al., 2019) to run an unperturbed control run and six perturbed ensemble members every 3 hours leading up to the event. The full model system (including data assimilation) was first spun up for 12 days in order for the surface and subsurface parameters to reach realistic values. The 13 members were initialized as follows: members 1–6 were initialized at 00 UTC, 2 Jun 2011, while members 7–12 and the unperturbed (control) member 0 were initialized three hours later (03 UTC), all well in advance of the event itself. A more detailed description of the model and its set-up is available in the Supporting Information S1.

2.2. The Pseudo-Global Warming Approaches

In a nutshell, similarly to the neutral case of Hibino et al. (2018) we adapted a PGW-approach (hereinafter PGW-Uni) that uses temperature, skin temperature and the sea surface temperature uniform anomalies added to the ECMWF's global IFS model driving data. Subsequently specific humidity was adjusted assuming relative humidity to be the same before and after the temperature adjustments. The anomalies used are -1°C , $+1^{\circ}\text{C}$, $+2^{\circ}\text{C}$ and $+3^{\circ}\text{C}$ according to the reference period of 1986–2005. The anomaly set of -1°C has been used creating a preindustrial “pseudo-warming” simulation. A more detailed justification for this choice is given in Section 3.2.

2.3. Risk Index of Exceeding Intensity Level: Proof of Concept

Several approaches were considered to compute the risk index of high precipitation using the information provided by the convection permitting NWP ensemble system. The simple way could be to look for each grid point at which percentage of the members has exceeded a selected threshold and define this as the risk index for this grid-point. This would, however, only represent the number of members reproducing such intensity, which would likely call for many more ensemble members to be of further use. Such an approach does not consider the model's limitations related to simulate the exact location of the event due to the inherent chaotic behavior of the convective system. To overcome this issue, we have developed a metric where we used a relaxed spatial criteria taking into account the neighboring grid cells of the specific grid point as discussed/proposed in Ben Bouallègue and Theis (2014). Using a neighborhood of grid points yields a probability that an event can happen somewhere in the neighborhood which is often more relevant to forecast and is common practice in met services. The size of the neighborhood is indeed ad-hoc and reflects both the domain of interest and a balance between the levels of hits and false alarms. In this metric, we have also relaxed the precipitation threshold since an explicit threshold may dampen the risk index for heavy precipitation artificially. The following steps describe how the risk index is computed. Note that to emphasize on the surrounding of Copenhagen, the risk index was computed inside the black square shown on Figure 2a.

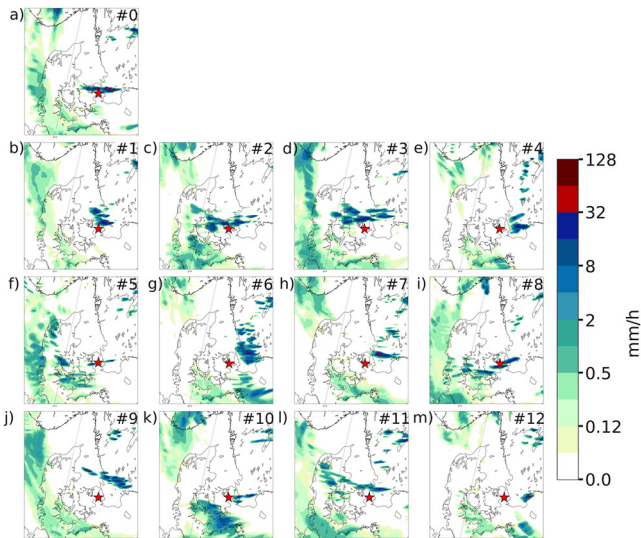


Figure: Accumulation of total precipitation from the control run (0) and the 12 perturbed members (1-12) for July 2, 2011 [16h00].

Figure 1. Hourly precipitation at 16 UTC for all members (a–m) for the control ensemble for 2 July 2011. The red star indicates the location of Copenhagen.

- For each point in a selected period of time (e.g., 1 hr) and ensemble member, if the precipitation rate t is higher or equal to a selected threshold T (e.g., 60 mm/hr), then the number one is assigned to the grid point for this members for this period.
- If the precipitation rate t is lower than the selected T (up to a minimum of $T-10$ mm for the selected period of time), then the number $e^{-\frac{(T-t)}{T}}$ is assigned to the grid point.
- Finally, if the first two conditions are not met for the grid point in concern, but it is in another grid cell within a radius of 40 km, the number $e^{-\frac{(T-t)}{T}} e^{-\frac{l}{L}}$ is assigned to the grid point where l is the distance from the selected grid point and the closet one where one of the two conditions being met and L is a e-folding distance chosen to be 150 km.
- The ensemble mean then defines the grid point risk index, where a value of 0 mean no risk and 1 the highest possible risk of occurrence.

The 40-km radius was chosen to be consistent with the city scale. More specifically, this choice was made to indicate the risk of an event hitting somewhere in the central, most densely populated part of Copenhagen. The 150 km distance representative of the scaled influenced (see e.g., Matte et al., 2021) of this kind of small-scale convective system. Due to the chaotic aspect of such small-scale heavy precipitation systems, an ensemble member could accidentally render a very high precipitation rate. In order to overcome this issue, the risks index have been computed using only 12 out of the 13 members, leaving out the member with the highest precipitation rate occurring within the black square shown on Figure 2a.

3. Results

3.1. Reference Simulations

The standard PGW approach was adapted because of its stabilizing effect on the convection mechanisms (see Section 3.2 for details). As discussed in the Supplementary Information, in terms of intensity and isolated structure, the event is well reproduced by the HARMONIE-AROME limited-area numerical weather prediction model. Although the exact location of the event is not well represented (due to the very chaotic behavior of cloudbursts), the very high intensities are correctly reproduced. Figure 1 shows an example of the hourly precipitation at 16 UTC (meaning the hourly accumulated precipitation from 15 UTC to 16 UTC, this definition is applied for the rest of the manuscript) for all members of the ensemble forecast. Some members (Figures 1a, 1b, 1e, and 1i) show an intensity quite similar to the observed (Figure S1c in Supporting Information S1); others show well located systems but at lower intensity (Figures 1c, 1f, and 1k); some completely fail in simulating both intensity and location in the clode vicinity of Copenhagen (Figures 1d, 1g, 1h, 1j, and 1l); while member #12 (Figure 1m) seems to have completely failed simulating any precipitation in the area. We should note that in terms of risk index, even if member #12 (Figure 1m) did not show signs of intense precipitation, it does not mean that the possibility of high precipitation rate for this member was nonexistent. This means that the synoptic and local preconditioning of the 16 UTC pattern is almost identical to that in the other members (not shown), but the sequence of processes have just unfolded differently for this member due to sensitivity to the initialization including that from assimilated observations. Figure 2 shows the computed risk index (see Section 2.3) in all ensemble members. The risk index for intense precipitation (see Figure 2h to see the associated risk index of Figure 1 using a 60 mm/hr threshold) is centered over Skåne (Scania, southern Sweden; see indications on Figure S4 in Supporting Information S1), but reaches the eastern part of Zealand in Denmark. The observed intensity over Copenhagen (see Section 1 of in Supporting Information S1) lends credibility to the computed risk index, despite an overall weak intensity over the city at that time.

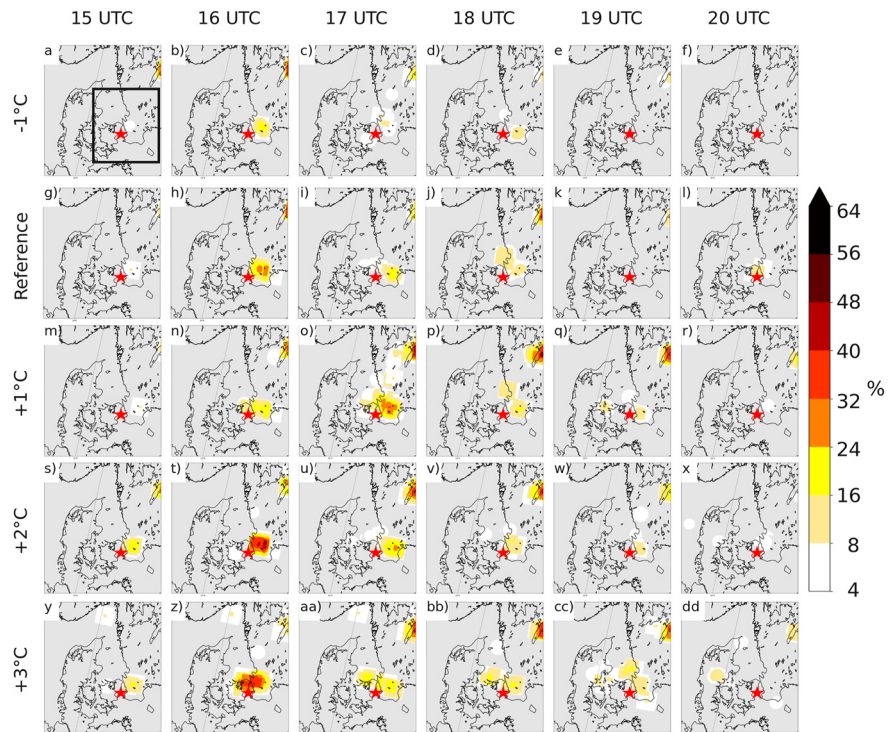


Figure 2. Risk index using a precipitation threshold of 60 mm/hr from 15 UTC to 20 UTC (columns) for all warming levels (a–f, m–r, s–x and y–dd for the -1°C , $+1^{\circ}\text{C}$, $+2^{\circ}\text{C}$ and $+3^{\circ}\text{C}$, respectively) and the reference case (g–l). The black square shown in panel (a) is the area used to produce Figure 3. The red star indicates the location of Copenhagen and the gray shading values under 4%.

3.2. The Adapted PGW Approach

A PGW approach (Schär et al., 1996) was applied to the ensemble simulation set-up in order to investigate the risk index of such an event under different warming levels. However, due to the very high sensitivity to IC of the event presented in this study, applying a PGW approach is not straightforward. This approach usually implies that the lateral boundary conditions (LBC) of the regional climate simulation are modified using long-term climate change anomalies inferred by coarse resolution climate model. So, the standard PGW approach (hereinafter PGW-GCM) uses large scale anomalies extracted from a GCM (Brogli et al., 2019; Liu et al., 2017; F. E. L. Otto, 2017). Although this method does not take into account changes in transient future patterns (Dai et al., 2020), it is implying to be a reflection of future mean warmer climate conditions. The advantages of using this approach are multiple, also involves some pitfalls as pointed out by Hibino et al. (2018). For example, Figure S5 in Supporting Information S1 is showing the same as Figure 1 but produced using a the standard PGW-GCM approach (see caption of Figure S5 in Supporting Information S1 for PGW-GCM set-up). At first glance, it becomes clear by comparing Figure S5 in Supporting Information S1 and Figure 1 that the structure of the precipitation patterns is quite different between the two ensembles while, from a synoptic perspective, the difference is not significant (not shown). The very small number of small weather systems (most likely convective systems) produced by the PGW-GCM is indicating that something is different in this set-up. An in-depth study of the convection mechanisms (not shown) suggest that the PGW-GCM has stabilized the atmosphere, killing then most of the convection mechanism necessary for generating this event, challenging an attribution analysis. This was also seen by Hibino et al. (2018).

In order to reproduce this event under warmer conditions, the characteristics that led to the original event must be maintained. In this view we have adopted, similar to the neutral case of Hibino et al. (2018), an additional PGW set up using this time a set of uniform anomalies (PGW-Uni, see Section 2.2). So, instead of using the anomalies deduced from a GCM, simplistic colder (-1°C) and warmer ($+1^{\circ}\text{C}$, $+2^{\circ}\text{C}$ and $+3^{\circ}\text{C}$) anomalies were added to the IC and the LBC from the driving data with the specific humidity adjusted to these warming levels. This latter set up differs from the PGW-GCM, since PGW-GCM anomalies are not horizontally and vertically homogeneous

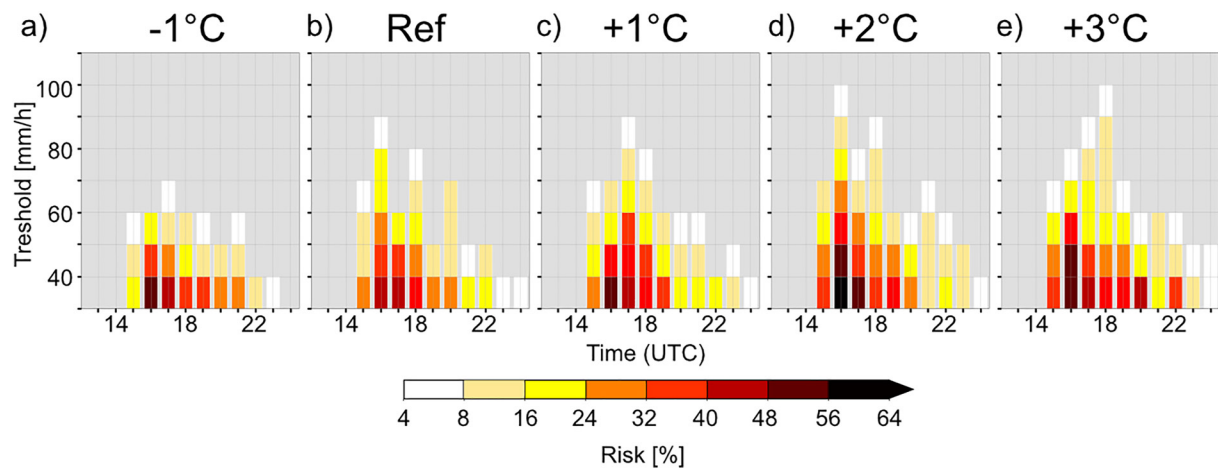


Figure 3. Time evolution of the max of the hourly risk index according to the precipitation threshold over the region of interest shown by the black square in Figure 2a. Panels (a–e) are provided from the warming levels -1°C , Ref, $+1^{\circ}\text{C}$, $+2^{\circ}\text{C}$ and $+3^{\circ}\text{C}$, respectively. The gray shading values under 4%.

over the domain. Since the main focus of this new experiment is to stay close to the original event, neither the pressure nor the winds were adjusted (tests using wind or no wind anomalies in the PGW-GCM approach showed no important impact on the investigated event, not shown). Figure S6 in Supporting Information S1 shows the same as Figure 1 but using the PGW-Uni where anomalies of 3°C are added. With this set-up, the 16 UTC precipitation patterns from PGW-Uni (Figure S6 in Supporting Information S1) are showing very similar patterns to Figure 1, which is much closer to what is depicted by the reference set-up while being more intense.

We acknowledge that the very straightforward anomalies used for PGW-Uni are not representative of the future climate let alone an average state, but keep the convective mechanism alive in warmer (and colder) conditions. On the other hand, while the mean state extracted from a GCM (or an ensemble mean) does reflect a plausible mean state of a warmer future, it most certainly does not represent conditions where such an event could take place. In short: adding an average state to a very unique and rare weather event does not necessarily make it more unique, just more average.

3.3. Storyline Approach

Using this PGW-Uni approach, we were able to assess the risk index, as previously defined, of high precipitation rate, which is shown in Figure 2. This figure shows that there are two regions that seem to reveal a risk index of intense precipitation (for the reference ensemble and all the warming levels): (a) one over Skåne and the Copenhagen area and (b) one over lake Vättern in Sweden. Note that the second region is also plausible according to the radar product (Figure S1 in Supporting Information S1), but did not lead to any major hazards. The second horizontal set of panels shows the risk index from the ensemble forecast of the present day reference, materializing at 15 UTC and peaking at 16 UTC and then dissipating toward the end of the day. Overall, a similar behavior is found in the other ensemble simulations although with different intensities.

An important aspect of Figure 2 is that the risk index is increasing with the temperature from cold to warmer levels. Specifically, comparing the ensemble representing the pre-industrial period (first row of Figure 2), one can see that the risk index of exceeding 60 mm/hr is reduced to about half of the reference ensemble (see second row of Figure 2) at the peak of the storm and furthermore the overall risk index for higher precipitation rates is also reduced (see Figures 3 and S8 in Supporting Information S1) by approximately a factor of two (from 29% to 17%, not shown). Since global temperature has increased by about 1°C since pre-industrial times (Masson-Delmotte et al., 2021), a proportion of the risk index produced by the reference ensemble could then be attributed to today's warmer conditions. As the climate warms, Figure 2 also show that the risk index is increasing while remaining more or less located over the same area (which is an indication the adapted PGW has not modified the impacted area).

The expected increase of the intense precipitation, as expected by a Clausius-Clapeyron scaling (i.e., an increase of $\approx 7\%$ of precipitation per degree of warming Trenberth et al., 2003), is also impacting the risk index of other thresholds as shown in Figures 3 and eight in Supporting Information S1. For example, if we look only at the evolution of the risk index at 16 UTC in Figure 3, we can see that not only does it increase for the same threshold (e.g., 60 mm/hr) but that it also appears at higher and higher precipitation thresholds as the climate warms from -1°C to $+2^\circ\text{C}$. Between $+2^\circ\text{C}$ and $+3^\circ\text{C}$, the risk index is not following this evolution. We rather identify a switch in time of the peak of risk index for higher precipitation rate with the overall risk index being similar between the two warmer ensembles (i.e., $+2^\circ\text{C}$ and $+3^\circ\text{C}$). This could be due (a) to an overall evolution of the storm thermodynamic mechanism at warmer levels producing more intense precipitation over a longer period inducing the risk index over a longer period of time or (b) to the ad hoc response from the chaotic nature of convective precipitation. We also note the same kind of increase with the impacted area by the risk index with warming. This agrees with previous studies (Christensen & Christensen, 2007; Frei et al., 1998; Matte et al., 2021; Prein, Liu, et al., 2017; Prein, Rasmussen, et al., 2017) showing that with an increased temperature, there is an increase of intense precipitation rates impacting the value of the risk index as computed in this study.

The increase in risk index is not systematic with the increasing thresholds for the intense precipitation rate which is also seen on Figure S8 in Supporting Information S1. For example, this latter figure shows that the risk index for low intensity such as 30 mm/3 hr is not increasing much as climate warms, while more intense precipitation rates do. We see that as climate warms, the risk index for higher precipitation rates do increase. Specifically, there is a risk of reaching precipitation amounts increasing from 100 mm/3 hr to 160 mm/3 hr when moving from the -1°C to $+3^\circ$ warming level.

4. Discussion

The cloud burst event of 2 July had a very localized but large impact upon the city of Copenhagen, which increased the awareness of the public and decision makers alike toward the effects of climate change and how to adapt city management for future potential high impact events. The task of producing a storyline on the risk of the 2 July cloudburst event to climate change is delicate. Using a simple Clausius-Clapeyron scaling (O’Gorman & Schneider, 2009), we could have expected an increase of 6%–7% of water content by an increment of 1°C of the surface temperature. However, such simple scaling is not appropriate for diagnosing the potential risk of already well known small-scale convective events and their potential impacts on society under warmer conditions. For example, any slight changes in the combination of sequences of atmospheric drivers might dampen or intensify the precipitation. Here, the mechanisms leading to the event were carefully maintained across several adapted PGW applications to emphasize the impact of different temperature levels by analyzing the associated risk index. The results of our study also suggest that the PGW approach is not straightforward and should not be applied blindly as the type of event, the anomalies used and the set-up in general (Brogli et al., 2019) will play out differently. Using our adapted PGW approach, we have shown that the risk for realizing precipitation amounts as in the actual event increases as climate warms, but also that the risk for even more intense precipitation rates is increasing.

Small-scale, heavy, flash floods such as the one presented in this study are unique, which makes the task of attributing them to climate change very challenging. For this type of event where the convective mechanisms are very strong and localized, the sensitivity to the vertical profile is very high, meaning that the application of stratification changes diagnosed from a mean change may not reflect the future climate day with a high potential for extreme precipitation or severe weather. In this study, we specifically chose to keep the vertical structure of the atmosphere the same in order to mimic the event observed in warmer conditions. In other words, the question is not what to expect for this type of event in the future (see e.g., Kahraman et al., 2021; Púčik et al., 2017; Rädler et al., 2019), but rather, given this extreme weather, what would happen if conditions were warmer with a similar synoptic configuration in the future. While this is outside the scope of this study, we acknowledge the need to understand related questions about extremes, such as studying the occurrence of convective hazard environments in a warmer climate.

Here, we have shown that an enhanced risk index (almost doubling) of exceeding the 60 mm/hr in the late afternoon in the 2011 Copenhagen case could be attributed to the warming of 1°C from pre-industrial conditions (approximately the current global warming Masson-Delmotte et al., 2021). As the lateral and IC get warmer, the

risk index is of longer duration and also increasing for unprecedented precipitation rates where +2°C and +3°C show similar risk index patterns suggesting a similar response to warming.

Data Availability Statement

The EC-EARTH-r3i1p1 RCP 8.5 simulation is available from the CMIP5 ESGF archive: <https://esgf-node.llnl.gov/projects/cmip5/>. Simulated precipitation fields are available from the Electronic Research Data Archive from the University of Copenhagen: <https://doi.org/10.17894/ucph.6cbaf65a-02b5-4087-a478-fa83f44e3b9d>.

Acknowledgments

J.H.C. conceived the idea. D.M. processed the model data, performed the analysis, led the writing, and produced the figures. D.M. and H.F. prepared the anomalies for the model initial conditions and lateral boundary conditions. H.F. realized the Harmonie model simulations. R.M.K.Z. produced graphics based on station precipitation measurements. All authors contributed to question the effect of an average PGW-GCM based change upon atmospheric stability when considering a particular, current time event. Finally, all participated to analyses, the discussion of the results and the writing of the paper. The authors are grateful to the two reviewers that helped improve this manuscript. We acknowledge funding by the European Union under the Horizon 2020 project EUCP (grant agreement 776613). The authors declare that they have no competing financial interests.

References

- Armon, M., Marra, F., Enzel, Y., Rostkier-Edelstein, D., Garfinkel, C. I., Adam, O., et al. (2022). Reduced rainfall in future heavy precipitation events related to contracted rain area despite increased rain rate. *Earth's Future*, *10*(1), e2021EF002397. <https://doi.org/10.1029/2021ef002397>
- Arnbjerg-Nielsen, K., Leonardsen, L., & Madsen, H. (2015). Evaluating adaptation options for urban flooding based on new high-end emission scenario regional climate model simulations. *Climate Research*, *64*(1), 73–84. <https://doi.org/10.3354/cr01299>
- Attema, J. J., Loriaux, J. M., & Lenderink, G. (2014). Extreme precipitation response to climate perturbations in an atmospheric mesoscale model. *Environmental Research Letters*, *9*(1), 014003. <https://doi.org/10.1088/1748-9326/9/1/014003>
- Bachmann, K., Keil, C., Craig, G. C., Weissmann, M., & Welzbacher, C. A. (2020). Predictability of deep convection in idealized and operational forecasts: Effects of radar data assimilation, orography, and synoptic weather regime. *Monthly Weather Review*, *148*(1), 63–81. <https://doi.org/10.1175/mwr-d-19-0045.1>
- Ben Bouallègue, Z., & Theis, S. E. (2014). Spatial techniques applied to precipitation ensemble forecasts: From verification results to probabilistic products. *Meteorological Applications*, *21*(4), 922–929. <https://doi.org/10.1002/met.1435>
- Bengtsson, L., Andrae, U., Aspelien, T., Batrak, Y., Calvo, J., de Rooy, W., et al. (2017). The HARMONIE-AROME model configuration in the ALADIN-HIRLAM NWP system. *Monthly Weather Review*, *145*(5), 1919–1935. <https://doi.org/10.1175/mwr-d-16-0417.1>
- Brogli, R., Kröner, N., Sørland, S. L., Lüthi, D., & Schär, C. (2019). The role of Hadley circulation and lapse-rate changes for the future European summer climate. *Journal of Climate*, *32*(2), 385–404. <https://doi.org/10.1175/jcli-d-18-0431.1>
- Christensen, J. H., & Christensen, O. B. (2007). A summary of the PRUDENCE model projections of changes in European climate by the end of this century. *Climatic Change*, *81*(1), 7–30. <https://doi.org/10.1007/s10584-006-9210-7>
- Coppola, E., Sobolowski, S., Pichelli, E., Raffaele, F., Ahrens, B., Anders, I., et al. (2020). A first-of-its-kind multi-model convection permitting ensemble for investigating convective phenomena over Europe and the Mediterranean. *Climate Dynamics*, *55*(1), 3–34. <https://doi.org/10.1007/s00382-018-4521-8>
- Dai, A., Rasmussen, R. M., Ikeda, K., & Liu, C. (2020). A new approach to construct representative future forcing data for dynamic downscaling. *Climate Dynamics*, *55*(1), 315–323. <https://doi.org/10.1007/s00382-017-3708-8>
- Fowler, H. J., Lenderink, G., Prein, A. F., Westra, S., Allan, R. P., Ban, N., et al. (2021). Anthropogenic intensification of short-duration rainfall extremes. *Nature Reviews Earth & Environment*, *2*(2), 107–122. <https://doi.org/10.1038/s43017-020-00128-6>
- Frei, C., Schär, C., Lüthi, D., & Davies, H. C. (1998). Heavy precipitation processes in a warmer climate. *Geophysical Research Letters*, *25*(9), 1431–1434. <https://doi.org/10.1029/98gl151099>
- Frogner, I.-L., Andrae, U., Bojarova, J., Callado, A., Escribà, P. A. U., Feddersen, H., et al. (2019). HarmonEPS—The HARMONIE ensemble prediction system. *Weather and Forecasting*, *34*(6), 1909–1937. <https://doi.org/10.1175/waf-d-19-0030.1>
- Hagelin, S., Son, J., Swinbank, R., McCabe, A., Roberts, N., & Tennant, W. (2017). The met office convective-scale ensemble, MOGREPS-UK. *The Quarterly Journal of the Royal Meteorological Society*, *143*(708), 2846–2861. <https://doi.org/10.1002/qj.3135>
- Hazeleger, W., van den Hurk, B. J. J. M., Min, E., van Oldenborgh, G. J., Petersen, A. C., Stainforth, D. A., et al. (2015). Tales of future weather. *Nature Climate Change*, *5*(2), 107–113. <https://doi.org/10.1038/nclimate2450>
- Hibino, K., Takayabu, I., Wakazuki, Y., & Ogata, T. (2018). Physical responses of convective heavy rainfall to future warming condition: Case study of the Hiroshima event. *Frontiers of Earth Science*, *6*, 35. <https://doi.org/10.3389/feart.2018.00035>
- Kahraman, A., Kendon, E. J., Chan, S. C., & Fowler, H. J. (2021). Quasi-stationary intense rainstorms spread across Europe under climate change. *Geophysical Research Letters*, *48*(13), e2020GL092361. <https://doi.org/10.1029/2020gl092361>
- Kawase, H., Imada, Y., Sasaki, H., Nakaegawa, T., Murata, A., Nosaka, M., & Takayabu, I. (2019). Contribution of historical global warming to local-scale heavy precipitation in western Japan estimated by large ensemble high-resolution simulations. *Journal of Geophysical Research: Atmospheres*, *124*(12), 6093–6103. <https://doi.org/10.1029/2018jd030155>
- Kawase, H., Imada, Y., Tsuguti, H., Nakaegawa, T., Seino, N., Murata, A., & Takayabu, I. (2020). The heavy rain event of July 2018 in Japan enhanced by historical warming. *Bulletin of the American Meteorological Society*, *101*(1), S109–S114. <https://doi.org/10.1175/bams-d-19-0173.1>
- Kawase, H., Yamaguchi, M., Imada, Y., Hayashi, S., Murata, A., Nakaegawa, T., et al. (2021). Enhancement of extremely heavy precipitation induced by Typhoon Hagibis (2019) due to historical warming. *SOLA, 17A-002*(Special_Edition), 7–13. <https://doi.org/10.2151/sola.17a-002>
- Khajehi, S., Ahmadi, A., Shao, W., & Moradkhani, H. (2020). A place-based assessment of flash flood hazard and vulnerability in the contiguous United States. *Scientific Reports*, *10*(1), 1–12. <https://doi.org/10.1038/s41598-019-57349-z>
- Lackmann, G. M. (2013). The south-central US flood of May 2010: Present and future. *Journal of Climate*, *26*(13), 4688–4709. <https://doi.org/10.1175/jcli-d-12-00392.1>
- Leach, N. J., Weisheimer, A., Allen, M. R., & Palmer, T. (2021). Forecast-based attribution of a winter heatwave within the limit of predictability. *Proceedings of the National Academy of Sciences*, *118*(49), e2112087118. <https://doi.org/10.1073/pnas.2112087118>
- Lenderink, G., de Vries, H., Fowler, H. J., Barbero, R., van Ulft, B., & van Meijgaard, E. (2021). Scaling and responses of extreme hourly precipitation in three climate experiments with a convection-permitting model. *Philosophical Transactions of the Royal Society A*, *379*(2195), 20190544. <https://doi.org/10.1098/rsta.2019.0544>
- Liu, C., Ikeda, K., Rasmussen, R., Barlage, M., Newman, A. J., Prein, A. F., et al. (2017). Continental-scale convection-permitting modeling of the current and future climate of north America. *Climate Dynamics*, *49*(1–2), 71–95. <https://doi.org/10.1007/s00382-016-3327-9>
- Loriaux, J. M., Lenderink, G., De Rooze, S. R., & Siebesma, A. P. (2013). Understanding convective extreme precipitation scaling using observations and an entraining plume model. *Journal of the Atmospheric Sciences*, *70*(11), 3641–3655. <https://doi.org/10.1175/jas-d-12-0317.1>

- Masson-Delmotte, V., Zhai, P., Priani, A., Connors, S. L., Péan, C., & Berger, S. (2021). IPCC, 2021: Climate Change 2021: The physical science basis. Contribution of working group I to the sixth assessment report of the intergovernmental panel on climate change.
- Matte, D., Christensen, J. H., & Ozturk, T. (2021). Spatial extent of precipitation events: When big is getting bigger. *Climate Dynamics*, 58(5–6), 1–15. <https://doi.org/10.1007/s00382-021-05998-0>
- National Academies of Sciences, Engineering, and Medicine. (2016). *Attribution of extreme weather events in the context of climate change*. National Academies Press.
- O’Gorman, P. A., & Schneider, T. (2009). The physical basis for increases in precipitation extremes in simulations of 21st-century climate change. *Proceedings of the National Academy of Sciences*, 106(35), 14773–14777. <https://doi.org/10.1073/pnas.0907610106>
- Olsson, J., Du, Y., An, D., Uvo, C. B., Sörensen, J., Toivonen, E., et al. (2021). An analysis of (sub-) hourly rainfall in convection-permitting climate simulations over southern Sweden from a user’s perspective. *Frontiers of Earth Science*, 9, 516. <https://doi.org/10.3389/feart.2021.681312>
- Otto, F., & Members of the Climate Science Communications Group. (2019). Attribution of extreme weather events: How does climate change affect weather? *Weather*, 74(9), 325–326. <https://doi.org/10.1002/wea.3610>
- Otto, F. E. L. (2017). Attribution of weather and climate events. *Annual Review of Environment and Resources*, 42(1), 627–646. <https://doi.org/10.1146/annurev-environ-102016-060847>
- Pall, P., Patricola, C. M., Wehner, M. F., Stone, D. A., Paciorek, C. J., & Collins, W. D. (2017). Diagnosing conditional anthropogenic contributions to heavy Colorado rainfall in September 2013. *Weather and Climate Extremes*, 17, 1–6. <https://doi.org/10.1016/j.wace.2017.03.004>
- Patricola, C. M., & Wehner, M. F. (2018). Anthropogenic influences on major tropical cyclone events. *Nature*, 563(7731), 339–346. <https://doi.org/10.1038/s41586-018-0673-2>
- Prein, A. F., Langhans, W., Fosser, G., Ferrone, A., Ban, N., Goergen, K., et al. (2015). A review on regional convection-permitting climate modeling: Demonstrations, prospects, and challenges. *Reviews of Geophysics*, 53(2), 323–361. <https://doi.org/10.1002/2014RG000475>
- Prein, A. F., Liu, C., Ikeda, K., Trier, S. B., Rasmussen, R. M., Holland, G. J., & Clark, M. P. (2017). Increased rainfall volume from future convective storms in the US. *Nature Climate Change*, 7(12), 880–884. <https://doi.org/10.1038/s41558-017-0007-7>
- Prein, A. F., Rasmussen, R. M., Ikeda, K., Liu, C., Clark, M. P., & Holland, G. J. (2017). The future intensification of hourly precipitation extremes. *Nature Climate Change*, 7(1), 48–52. <https://doi.org/10.1038/nclimate3168>
- Prein, A. F., Rasmussen, R. M., Wang, D., & Giangrande, S. E. (2021). Sensitivity of organized convective storms to model grid spacing in current and future climates. *Philosophical Transactions of the Royal Society A*, 379(2195), 20190546. <https://doi.org/10.1098/rsta.2019.0546>
- Pučík, T., Groenemeijer, P., Rädler, A. T., Tijssen, L., Nikulin, G., Prein, A. F., et al. (2017). Future changes in European severe convection environments in a regional climate model ensemble. *Journal of Climate*, 30(17), 6771–6794. <https://doi.org/10.1175/jcli-d-16-0777.1>
- Rädler, A. T., Groenemeijer, P. H., Faust, E., Sausen, R., & Púčik, T. (2019). Frequency of severe thunderstorms across Europe expected to increase in the 21st century due to rising instability. *NPJ Climate and Atmospheric Science*, 2(1), 1–5. <https://doi.org/10.1038/s41612-019-0083-7>
- Ricchi, A., Bonaldo, D., Cioni, G., Carniel, S., & Miglietta, M. M. (2021). Simulation of a flash-flood event over the Adriatic Sea with a high-resolution atmosphere-ocean-wave coupled system. *Scientific Reports*, 11(1), 1–11. <https://doi.org/10.1038/s41598-021-88476-1>
- Schär, C., Frei, C., Lüthi, D., & Davies, H. C. (1996). Surrogate climate-change scenarios for regional climate models. *Geophysical Research Letters*, 23(6), 669–672. <https://doi.org/10.1029/96gl00265>
- Schellander-Gorgas, T., Wang, Y., Meier, F., Weidle, F., Wittmann, C., & Kann, A. (2017). On the forecast skill of a convection-permitting ensemble. *Geoscientific Model Development*, 10(1), 35–56. <https://doi.org/10.5194/gmd-10-35-2017>
- Shepherd, T. G., Boyd, E., Calel, R. A., Chapman, S. C., Dessai, S., Dima-West, I. M., et al. (2018). Storylines: An alternative approach to representing uncertainty in physical aspects of climate change. *Climatic Change*, 151(3), 555–571. <https://doi.org/10.1007/s10584-018-2317-9>
- Takayabu, I., Hibino, K., Sasaki, H., Shiogama, H., Mori, N., Shibutani, Y., & Takemi, T. (2015). Climate change effects on the worst-case storm surge: A case study of Typhoon Haiyan. *Environmental Research Letters*, 10(6), 064011. <https://doi.org/10.1088/1748-9326/10/6/064011>
- Trenberth, K. E., Dai, A., Rasmussen, R. M., & Parsons, D. B. (2003). The changing character of precipitation. *Bulletin of the American Meteorological Society*, 84(9), 1205–1218. <https://doi.org/10.1175/bams-84-9-1205>

References From the Supporting Information

- Bénard, P., Vivoda, J., Mašek, J., Smolíková, P., Yessad, K., Smith, C., et al. (2010). Dynamical kernel of the Aladin-NH spectral limited-area model: Revised formulation and sensitivity experiments. *Quarterly Journal of the Royal Meteorological Society*, 136(646), 155–169. <https://doi.org/10.1002/qj.522>
- Bouttier, F., Raynaud, L., Nuissier, O., & Ménétrier, B. (2016). Sensitivity of the AROME ensemble to initial and surface perturbations during HyMex. *Quarterly Journal of the Royal Meteorological Society*, 142(S1), 390–403. <https://doi.org/10.1002/qj.2622>
- Brousseau, P., Berre, L., Bouttier, F., & Desroziers, G. (2011). Background-error covariances for a convective-scale data-assimilation system: AROME-France 3D-Var. *The Quarterly Journal of the Royal Meteorological Society*, 137(655), 409–422. <https://doi.org/10.1002/qj.750>
- Cuxart, J., Bougeault, P., & Redelsperger, J. (2000). A turbulence scheme allowing for mesoscale and large-eddy simulations. *Quarterly Journal of the Royal Meteorological Society*, 126(562), 1–30. <https://doi.org/10.1002/qj.49712656202>
- Ebisuzaki, W. L. N. A. Y., & Kalnay, E. (1991). Ensemble experiments with a new lagged average forecasting scheme. In *WMO Research Activities in Atmospheric and Oceanic Modeling Report* (Vol. 15, p. 308).
- Lenderink, G., & Holtlag, A. A. M. (2004). An updated length-scale formulation for turbulent mixing in clear and cloudy boundary layers. *Quarterly Journal of the Royal Meteorological Society*, 130(604), 3405–3427. <https://doi.org/10.1256/qj.03.117>
- Masson, V., Le Moigne, P., Martin, E., Faroux, S., Alias, A., Alkama, R., et al. (2013). The SURFEXv7. 2 land and ocean surface platform for coupled or offline simulation of earth surface variables and fluxes. *Geoscientific Model Development*, 6(4), 929–960. <https://doi.org/10.5194/gmd-6-929-2013>
- Seity, Y., Brousseau, P., Malardel, S., Hello, G., Bénard, P., Bouttier, F., et al. (2011). The AROME-France convective-scale operational model. *Monthly Weather Review*, 139(3), 976–991. <https://doi.org/10.1175/2010mwr3425.1>
- Simmons, A. J., & Burridge, D. M. (1981). An energy and angular-momentum conserving vertical finite-difference scheme and hybrid vertical coordinates. *Monthly Weather Review*, 109(4), 758–766. [https://doi.org/10.1175/1520-0493\(1981\)109<0758:aeaamc>2.0.co;2](https://doi.org/10.1175/1520-0493(1981)109<0758:aeaamc>2.0.co;2)
- Woetmann, N. A. (2011). Downpour in Copenhagen on July 2, 2011. *Vejret*, 128, 12–22.